Computer Methods and Programs in Biomedicine (2004) **76**, 193—206

ELSEVIER

Computer Methods and Programs in Biomedicine

www.intl.elsevierhealth.com/journals/cmpb

Simulating growth dynamics and radiation response of avascular tumour spheroids—model validation in the case of an EMT6/Ro multicellular spheroid

Evangelia I. Zacharaki[a,*], Georgios S. Stamatakos[b,1], Konstantina S. Nikita[a,2], Nikolaos K. Uzunoglu[a,3]

[a] *School of Electrical and Computer Engineering, Division of Information Transmission Systems and Materials Technology, National Technical University of Athens, 9, Iroon Polytechniou, GR-15780 Zografos, Greece*
[b] *School of Electrical and Computer Engineering, Institute of Communication and Computer Systems, National Technical University of Athens, 9, Iroon Polytechniou, GR-15780 Zografos, Greece*

Received 11 June 2004; accepted 5 July 2004

KEYWORDS
Simulation;
Tumour growth;
Radiation therapy;
EMT6 spheroid;
Surviving fraction;
Cancer

Summary The goal of this paper is to provide both the basic scientist and the clinician with an advanced computational tool for performing in silico experiments aiming at supporting the process of biological optimisation of radiation therapy. Improved understanding and description of malignant tumour dynamics is an additional intermediate objective. To this end an advanced three-dimensional (3D) Monte-Carlo simulation model of both the avascular development of multicellular tumour spheroids and their response to radiation therapy is presented. The model is based upon a number of fundamental biological principles such as the transition between the cell cycle phases, the diffusion of oxygen and nutrients and the cell survival probabilities following irradiation. Efficient algorithms describing tumour expansion and shrinkage are proposed and applied. The output of the biosimulation model is introduced into the (3D) visualisation package AVS-Express, which performs the visualisation of both the external surface and the internal structure of the dynamically evolving tumour based on volume or surface rendering techniques. Both the numerical stability and the statistical behaviour of the simulation model have been studied and evaluated for the case of EMT6/Ro spheroids. Predicted histological structure and tumour growth rates have been shown to be in agreement with

* Corresponding author. Tel.: +30 210 77229 68; fax: +30 210 77235 57.
E-mail addresses: ezachar@biosim.ntua.gr (E.I. Zacharaki), gestam@central.ntua.gr (G.S. Stamatakos), knikita@cc.ece.ntua.gr (K.S. Nikita), nuzu@cc.ece.ntua.gr (N.K. Uzunoglu).
[1] Tel.: +30 210 772 22 88; fax: +30 210 772 35 57.
[2] Tel.: +30 210 772 22 85; fax: +30 210 772 35 57.
[3] Tel.: +30 210 772 35 56; fax: +30 210 772 35 57.

0169-2607/$ — see front matter
doi:10.1016/j.cmpb.2004.07.003

published experimental data. Furthermore, the underlying structure of the tumour spheroid as well as its response to irradiation satisfactorily agrees with laboratory experience.

1. Introduction

Radiation therapy (external beam therapy, brachytherapy) is applied to cancer patients each year as therapy or for palliation, or as an adjunct to surgery or chemotherapy. In order to achieve the best outcome for the patient in terms of tumour control and complication frequency, an optimisation process of the treatment planning should take place before the radiation delivery. As cancer biology is one of the most crucial determinants of the treatment outcome, efficient modelling, simulation and visualisation of the biological phenomena taking place before, during and after irradiation is of paramount importance. The practical usefulness of such processes is both to improve understanding of the cancer behaviour and to optimise the spatiotemporal treatment plan by performing in silico (= on the computer) experiments before the actual delivery of radiation to the patient. The objective function concerning exclusively tumour control can be the overall tumour repopulation (number of surviving tumour cells). Optimisation aims at minimising tumour repopulation for the maximum possible duration. In the clinical setting a compromise between minimisation of tumour repopulation for the maximum possible duration and minimisation of healthy tissue damage (including early and late normal tissue cell loss) is sought.

The objective of this paper is to demonstrate how algorithm and complexity theory, the generic Monte-Carlo stochastic technique and current visualisation tools can be combined in order to efficiently simulate the growth and response to irradiation of three-dimensional (3D) multicellular tumour spheroids. The biophysical part of the proposed approach is based on a discrete time cell cycle model, which is applied to each one of the cells constituting the tumour. The discrete time and space character of such a model allows the imposition of arbitrary boundary conditions such as the spatial profile of the oxygen and glucose supply. Therefore, this kind of model can be easily extended to the in vivo case [1], where the presence of different tissues producing variable elastic and nutrient supply profiles in the vicinity of a tumour can greatly affect the growth pattern. Furthermore, simulation of the growth of a multifocal tumour or a tumour of arbitrary geometry can be readily performed. Special emphasis is placed on the adjustment of the model output to experimental data. To this end, some previous model assumptions [1] have been modified in order to refine the description of the involved phenomena. Although the present paper does not deal with the damage to healthy tissue, our group is currently working on the development of an analogous computer model simulating the response of both hierarchical and flexible normal tissue systems to irradiation. A more simplistic approach of quantifying the effect to irradiation to healthy tissues could be the application of the concept of normal tissue complication probability (NTCP).

The paper begins with a brief description of the most essential assumptions concerning cell division and interaction. A number of novel algorithms describing expansion and shrinkage of the entire tumour system are presented and the space-time quantization policy is clarified. As an application example, the case of EMT6/Ro tumour spheroid in vitro is considered. Franko et al. [2] showed that EMT6 spheroids appear to satisfactorily model the response of EMT6 tumours to irradiation. Both the numerical stability and the statistical behaviour of the model predictions are checked. The predicted histological structure and the tumour growth rates are compared with published experimental data. Subsequently, the response of the heterogeneous population of the spheroid tumour system according to the nutrient deprivation is simulated by using the linear quadratic (LQ) model [3]. Different fractionation schemes are simulated and both the external and the internal structure of the spheroids are 3D visualised. Qualitative agreement with both experiment and clinical experience concerning the application of fractionated irradiation strengthens the robustness of the model as a decision and treatment planning supporting system.

2. Background

Multicellular tumour spheroids are characterized by the emergence of cellular heterogeneity and can constitute a satisfactory in vitro model of solid tumours [4]. Therefore, a substantial volume of experimental work on tumour spheroids investigating

basic biological mechanisms, such as metabolism and proliferation, regulation of growth saturation, differentiation and development of necrosis has been performed during the last decades [5—7]. Due to the particular structural characteristics of tumour spheroids, cell to cell interactions are facilitated. Such interactions may modify the cellular metabolism and thus the response to therapy.

While experimental [8—10] and mathematical [11—13] models dominate the field of tumour research, a relatively limited number of computer modelling approaches has appeared in the literature. The main purpose of such models is to perform virtual in silico experiments aiming at optimising the various cancer treatment modalities. Such models have been used in order to study, e.g. the evolution of a spheroidal tumour in nutrient medium [14—16], the growth and behaviour of a tumour in vivo [17—19], the neovascularisation (angiogenesis) process [20], the competition between neoplastic and immune subsystems [21] etc. Moreover, computer simulation models aim at three-dimensionally predicting and visualising the response of a tumour to various schemes of radiation therapy with respect to time. Duechting [22] developed a three-dimensional simulation model of tumour response to irradiation by combining systems analysis and cellular automata. Ginsberg [23] described the growth of an exactly spherical multilayer tumour in vitro by applying general control theory methods and appropriate commercial software. Nahum and Sanchez-Nieto [24] presented a computer model based on the concept of the tumour control probability (TCP) and studied TCP as a function of the spatial dose distribution. Stamatakos et al. [1,15,19] developed a three-dimensional discrete radiation response model of a tumour both in vitro and in vivo and introduced high performance computing and virtual reality techniques in order to visualise the external surface and the internal structure of a dynamic tumour. Kocher et al. developed a simulation model of tumour response to fractionated radiotherapy [25] and radiosurgery (single dose application) [26] and studied the vascular effects.

3. Design considerations

A reliable tool to theoretically study the effect of the various parameters on the progression of malignant tumours and their response to therapeutic interventions would substantially facilitate the work of the basic scientist. Besides, the in silico produced knowledge would contribute to gaining both qualitative and quantitative insight into the underlying biological phenomena.

On the other hand, the clinician needs a reliable platform in order to optimise treatment planning based on the individual patient's data, e.g. the particular histopathology and the genetic profile that determines the radiobiological parameters of the LQ model. As already mentioned tumour spheroids have proved to be the most reliable in vitro models of clinical tumours in vivo. Furthermore, experimenting in silico with small avascular micrometastases is expected to enhance the effectiveness of treatment concerning local invasion.

The systems design aims at satisfying the abovementioned requirements.

4. Theory and computational methods

The model formulation is based on the cellular level. Angiogenesis is not taken into account. This is a plausible hypothesis for both tumour growth in cell culture and the non-vascularised tumour or metastatic nodule growth in vivo. In the following, the model assumptions based on previous work with eventual modifications [1,15,16] are presented. The diagram describing the overall computational procedure is shown in Fig. 1.

4.1. Tumour growth kinetics

1. The cytokinetic model shown in Fig. 2 is adopted. According to this model, a tumour cell, when cycling, passes through the phases G_1 (gap 1), S (DNA synthesis), G_2 (gap 2) and M (mitosis). After mitosis is completed, each one of the resultant cells re-enters G_1 if oxygen and nutrient supply in its current position is adequate. Otherwise, it enters the resting G_0 phase. It should be noted that although from the purely biological point of view each ''mother'' cell disappears through mitosis and two equivalent ''daughter'' cells appear in its place, in this paper the convention of considering one ''mother'' and one ''daughter'' cell has been adopted.
2. A cell in the G_0 phase is not actively synthesizing DNA but may have become arrested in the G_1, S or G_2 phase of the cell cycle [27]. It stays in the G_0 phase for as long as its distance (r) to glucose and oxygen supply is greater than the thickness of the proliferating cell layer (T_P) and lower than the thickness of the viable cell layer (T) (Fig. 3). If the local environment of the cell becomes adequate ($r < T_P$) the cell re-enters G_1. Conversely a cell, deprived of oxygen or glucose ($r > T$),

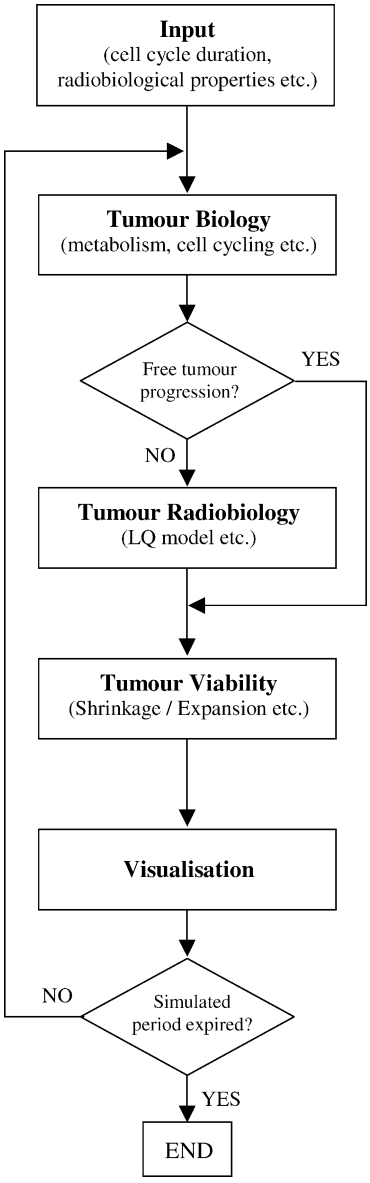

Fig. 1. Schematic diagram of the overall computational procedure.

looses its energy-producing capacity and enters necrosis (N) [28]. The thickness of the viable rim decreases linearly as a function of the spheroid diameter [28,29]. The thickness decrease could be explained by two factors. The first one is the reduction of the surface-to-volume ratio, which influences the nutrient-supply mechanism. The second one is the action of cytostatic factors diffusing out of the necrotic core [30]. The growth inhibitory factors reduce the number of proliferating cells and the viability inhibitors affect the viability of cells near the necrotic core [28]. As the proliferating cell layer is part of the viable rim, the same decrease rate for T_P has been assumed. The thickness of the hypoxic cell layer (T_{G_0}) can be calculated as the difference of the viable and the proliferating cell rim.

3. In addition to, the previously described pathway, there is always a probability that each cell residing in any phase (other than necrosis or apoptosis) dies with some probability per hour due to both ageing and spontaneous apoptosis (SA). This probability representing the cell loss rate due to apoptosis is the product of the cell loss factor due to apoptosis (with a typical value of, e.g. 10%) and the cell birth rate [3]. The cell birth rate can be considered as the ratio of the growth fraction (with a typical value of, e.g. 40%) [3,27] to the cell cycle duration.

4.2. Tumour geometry

1. A 3D mesh discretizing the volume occupied by the cell culture is used. This volume includes the tumour as well as part of the surrounding nutrient medium. Each cubic geometrical cell of the mesh can be occupied by a vital tumour cell (Fig. 4), by products of cell death (either necrotic or apoptotic) or by the nutrient medium.
2. The total space occupied by the simulated cell culture has been confined to 120 × 120 × 120 mesh cells. This limit depends on the available computer memory and power as well as on the maximum tolerable runtime.
3. The tumour spheroid formation starts with the placement of either a single tumour cell at the stage of mitosis or a small tumour spheroid at the centre of the discretizing mesh. A tumour cell can divide even if there is no free space for the daughter cell to be accommodated.
4. Communication between cells at any angular direction is possible.
5. The cell lysis and apoptosis products are gradually diffused towards the outer environment of the tumour. In case of in vivo tumour growth, such substances are expected to be partly ingested by phagocytes. In this case, the macroscopic result of this mechanism is tumour shrinkage due to the exertion of external pressures. Tumour shrinkage is computationally achieved by shifting a cell chain from the external environment of the tumour towards the cell that has to disappear in a direction defined by the cell and the centre of the mesh. In this way tumour connectivity is preserved, because all cells tend to move towards the centre of the tumour. Tumour expansion is computationally achieved by shifting a cell chain from the newly occupied mesh cell towards the external environ-

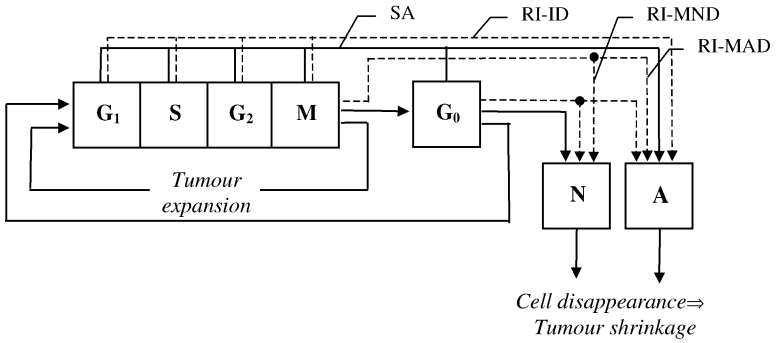

Fig. 2. Cytokinetic model of a tumour cell. The solid lines represent cell proliferation and cell death without application of any therapeutic treatment. The dashed lines represent the cell response to irradiation. Symbol explanation: G_1: G_1 phase, S: DNA synthesis phase, G_2: G_2 phase, G_0: G_0 phase, N: necrosis, A: apoptosis, SA: spontaneous apoptosis, RI: radiation induced, ID: interphase death, MND: mitotic necrotic death, MAD: mitotic apoptotic death.

ment of the tumour in a random direction. The shifting direction is defined in spherical coordinates using two random numbers that define the azimuthal angle in the *xy*-plane and the *z*-coordinate in the *z*-axis. In both cases, i.e. tumour expansion and shrinkage, integer rounding is applied to determine the best possible sequence of cells that has to be shifted in the discretizing mesh (Fig. 4).

4.3. Time quantization and statistical behaviour of the phase durations

1. Time is quantized and measured in appropriate units. In this paper, 1 h has been adopted as the unit of time.
2. The durations of the various cell states follow normal (Gaussian) distribution.
3. The simulation can be considered a row-to-row computation of the cell algorithm for each individual cell. At each time step, the remaining time in the current phase of the cell under examination is reduced by one time unit. The configuration obtained in this way serves as the initial step of the subsequent calculation step.

4.4. Tumour cell response to irradiation

1. The response of each cell to irradiation, leading to absorbed dose *d* is described by the LQ model [31]. According to this model, the survival probability *S*(*d*) of the cell is given by the expression

$$S(d) = \exp[-(\alpha d + \beta d^2)], \quad (1)$$

where α and β are parameters describing the radiobiological properties of the specific tumour [3]. It is noted that Eq. (1) is effective after the

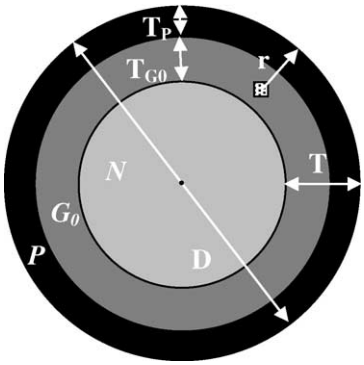

Fig. 3. Parameter definition in the spheroid model. P: proliferating cells, G_0: quiescent cells, N: necrosis. *T*: thickness of the viable cell layer, T_P: thickness of the proliferating cell layer, T_{G_0}: thickness of the hypoxic cell layer, $T_{G_0} = T - T_P$, *D*: spheroid diameter, *r*: distance of an arbitrary cell to glucose and oxygen supply.

expiration of a time interval sufficient for the sublethal damage to be repaired (i.e. 4 h after irradiation).
2. Cells in any cell cycle phase are more radiosensitive than hypoxic cells residing in G_0. Cells in the

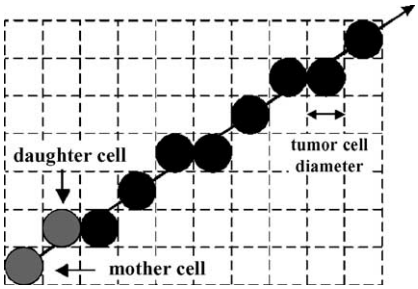

Fig. 4. The best possible approximation of an ideal line given a discretizing mesh (shown for simplicity in two-dimensions). The algorithm is applied to the modelling of tumour expansion.

S phase are more radioresistant than cells in any other cycle phase (G_1, G_2 and M). Three different sets of values for the α and β parameters of the LQ model are assumed: one set for the proliferating cell cycle phases except the S phase (α_P, β_P), a second one for the S phase (α_S, β_S) and a third one for the resting G_0 phase (α_{G_0}, β_{G_0}). This assumption is justified by the experimentally established different values of radiosensitivity in the above-mentioned phases [32,33]. The radiobiological parameters of the tumour cells (α and β parameters of the LQ model) are obtained by fitting the LQ model to an experimental survival curve. However these values are often not very accurate, as ''trade-off'' between α and β allows a range of combinations of the two parameters to fit the data almost equally well. A useful alternative for the calculation of the linear component of cell killing is to use low dose rate irradiation. The cell survival curve at low dose rate seems to extrapolate the initial slope of the high dose rate curve [3].

3. The cell death due to irradiation is simulated by three mechanisms: the radiation induced interphase death (RI-ID), the radiation induced mitotic necrotic death (RI-MND) and the radiation induced mitotic apoptotic death (RI-MAD) [34,35]. These distinct pathways are shown in Fig. 2. Notwithstanding the fact that quantitative data concerning the above-mentioned discrete mechanisms are rare or even non existent, estimates of a rather qualitative character have been published. In this work, the following assumptions characterised by a reasonable quantification of rather qualitative experimental observations have been made. Each irradiated cell residing in the G_0 phase that will not survive according to the LQ model can die by either apoptosis (with a 20% probability) or necrosis (with an 80% probability). Cycling cells being exposed to ionising radiation can die either before entering division or after having completed mitosis. The first form of death takes place through apoptosis (interphase death, with a 20% probability) whereas the second one, occurring after several divisions (e.g. three), may be associated with either apoptosis (mitotic apoptotic death, 10% probability) or necrosis (mitotic necrotic death, 70% probability). During each division the resultant ''daughter'' cell is identical to the ''mother'' cell, i.e. it is damaged by radiation. The probability of occurrence of mitotic death has been assumed much higher than the probability of interphase death as for the most cell lines in vitro the primary form of cell death is associated with mitosis [34].

5. System description

The Visual Fortran 6.0 programming language has been used for the model formulation. A typical simulation run of 5 weeks for 120 × 120 × 120 geometrical cells takes about 5 min on an AMD Athlon XP 1800 machine (786 MB RAM). The equatorial sections of the simulated tumour spheroid are visualised in two-dimensions using the standard software package MATLAB. The 3D visualisation of the predictions of the suggested simulation model is facilitated by software from Advanced Visual Systems (AVS). AVS/Express™ provides utilities for medical data acquisition, volume and surface rendering of human body regions of interest and 3D data manipulation functionalities like intersection of data in different cutting planes and orientations. AVS Express™ enables users to acquire input data sets from the output of tumour growth simulation software and create 3D models of the tumour geometry. The AVS/Express-based application allows the user to simulate the placement and the superposition of the different cell states and combine them into a single 3D representation. The visualised volumes of three cell states (proliferating, dormant and necrotic/apoptotic) are combined into a single 3D scene, since the use of colouring and transparency enables the visualisation of complex cell topologies. The final representation obtained can be exported from the AVS in VRML 1.0 or 2.0 formats and become available for study in a machine independent and interoperable way for local or remote examination through a local network or the Internet.

6. Status report

In the following application, details and representative results concerning the cases of an EMT6/Ro-tumour spheroid (mammary sarcoma of the mouse) are given, as the EMT6 spheroids are very often used in therapy-related experimentation.

6.1. Tumour growth

6.1.1. Simulation robustness

Random numbers have proved to be very useful in the solution of computationally complex problems or in the simulation of systems under different starting or operating conditions. Appropriate pseudo-random number generators are used in order to simulate the statistical character of specific biological phenomena during cell proliferation and irradiation. In order to identify the effect of the use

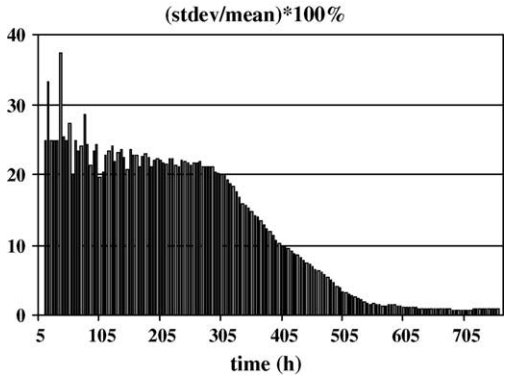

Fig. 5. Ratio of the standard deviation (stdev) to the mean value of the tumour volume using five different random number generator seeds. The simulation procedure starts with a single tumour cell.

of random numbers on the model accuracy and robustness, five different seeds for the random number generator have been investigated for the case of an EMT6-spheroid. The ratio of the standard deviation (stdev) to the mean value of the tumour volume is calculated as a function of time.

If a simulation of tumour growth begins with a single tumour cell placed at the centre of the nutrient medium, the standard deviation of the total tumour volume can be as high as 30% of the mean value (Fig. 5). This is expected because of the small mean value of the tumour volume at the beginning of the process. Nevertheless, after 650 simulated hours, the standard deviation of the total tumour volume decreases to less than 1% of its mean value (Fig. 5). In order to investigate the influence of random processes in the early stages of tumour growth, the simulated tumour spheroid formation has been started with the placement of a small multicellular tumour spheroid with varying number of cells. By initializing the simulation procedure with a multicellular spheroid of 122,000 cells, which corresponds to a tumour formed 400 simulated hours after the placement of a single clonogenic cell in the nutrient medium, it has been observed that the standard deviation of the total tumour volume is always less than 1.3%. The small statistical error determined with both initialisations renders the predictions sufficiently reliable in both cases. It should be stressed that the above presented expansion and shrinkage algorithms have provided the highest numerical stability in the simulation model when compared with the corresponding algorithms previously investigated by our group [15].

6.1.2. Geometry

As already described, the discretizing mesh consists of cubic geometrical cells, each one including a single tumour cell as well as the corresponding intracellular medium. As the tumour cells are closely packed, the edge of any given geometrical cell is assumed to approximate the tumour cell diameter (d_C) (Fig. 4). Hence the volume of the geometrical cell is d_C^3. The geometrical cell volume is assumed to have the same value everywhere within the spheroid and at any instant during spheroid growth. The tumour spheroid diameter (D) is calculated according to the equation

$$D = 2\sqrt[3]{\frac{3}{4\pi}N \cdot d_C^3}, \tag{2}$$

where N is the number of the geometrical cells occupied by the tumour spheroid.

The tumour cell diameter can be calculated from the tumour cell volume. As a typical mean cell volume in EMT6/Ro spheroids is 2500 μm^3 [36], the mean cell diameter has been calculated to be d_C = 16.8 μm. The tumour cell diameter is used as an adjusting parameter in order to express the values defined in real dimensions (e.g. in μm) in terms of the number of cells as in the case of the rim thickness.

The thickness T of the viable cell layer tends to behave as a linear function of the spheroid diameter D. The slope of the thickness depends on the glucose concentration and typically varies between -0.017 and -0.052 in the case of EMT6/Ro spheroids [28]. The corresponding equation is

$$T(D) = -0.025D + T_0, \tag{3}$$

where T_0 is a constant depending on the spheroid diameter (D_I) at which necrosis first develops. The units of D, T and T_0 must all be the same (i.e. μm). The following property must be satisfied for the diameter D_I [28]:

$$D_I = 2T(D_I) \tag{4}$$

According to (3) and (4)

$$T_0 = 0.525D_I \tag{5}$$

The onset of necrosis depends on the nutrient concentration. Under normal conditions (0.28 oxygen and 5.5 mM glucose concentration) necrosis initially develops at a diameter of $\sim$400 μm, resulting in T_0 = 210 μm. The thickness of the proliferating cell layer has been assumed to be $T_P(D) = -0.025D + T_{P0}$. According to [23,36] the spheroid diameter at which hypoxia first develops is $\sim$300 μm in EMT6/Ro spheroids. In the same way T_{P0} is calculated (T_{P0} = 157.5 μm).

Table 1 Rounded mean values and standard deviations of the phase durations for EMT6 tumour cells

Cell phase	N (h)	A (h)	G_1 (h)	S (h)	G_2 (h)	M (h)
Mean duration	40[a]	0[a]	6	10	2	2
Standard deviation	2	2	1	2	0	0

N: necrosis; A: apoptosis; G_1: gap 1 phase; S: synthesis; G_2: gap 2 phase; M: mitosis.

[a] Extra duration due the diffusion of the necrotic/apoptotic products: 10 h.

Table 2 Comparison of the experimental with the simulated extent of central necrosis as a function of the spheroid diameter

Spheroid diameter (μm)	Experimental (%)	Simulated[a] (%)
468	>1	0.4
821	12	18
1156	28	32
1347	38	39

[a] Necrotic volume/total volume) × 100%. The apoptotic products constituting approximately 1.2% of the total tumour volume have not been taken into account.

6.1.3. Results

Typical mean values and standard deviations of the phase durations of the constituting cells for the EMT6-spheroid are shown in Table 1 [23]. Fig. 6a shows the total number of viable cells of a multicellular tumour spheroid of a mammary sarcoma of the mouse grown in cell culture as a function of the growth time. The Gompertzian pattern of tumour growth is explained by the absence of blood vessels in cell cultures. Fig. 6b shows the spheroid diameter of the same spheroid as a function of time. The growth curves have been redrawn from Freyer et al. [36] with permission. Fig. 6c and d show the simulation data of the volumetric growth and the spheroid diameter, respectively. All results represent the mean values of three simulation runs each one having different seed of the random number generator. Both predictions agree very well with the experimental results for the time interval under consideration. Nevertheless, the calculated spheroid diameter of the simulated tumour does not increase linearly with time, as is the experimental case. This could be explained by the assumption of a constant cell volume. According to [36] the cell volume decreases from 3100 to 1600 μm^3 at a diameter of 1500 μm. This means that our mean value of 2500 μm^3 for the cell volume underestimates the spheroid diameter in the early stages of growth and overestimates it in the later stages of growth.

The cell cycle duration and the time required for cell death and tumour shrinkage determine the temporal evolution of the spheroid. As expected, the volume growth becomes saturated over time. The mechanism simulating the spheroid saturation can be described as a modulation of the spheroid size. As the spheroid is growing, the viable rim decreases and some cells become necrotic. Subsequently, the necrotic products are diffused which practically means they are disappearing and the tumour shrinks. As the tumour is shrinking the proliferating rim is increasing and some dormant cells re-enter the cell cycle. This process results again in tumour expansion. If the rim were constant, i.e. independent of the spheroid diameter, the tumour growth rate would decrease with time as the percentage of the proliferating cells is decreasing. In such a case, although the initial stages of the Gompertzian growth are satisfactorily simulated, the growth saturation stage tends to be poorly predicted [1,15].

Table 2 presents the portion of central necrosis in the total tumour volume as a function of the spheroid diameter. The simulation data have been compared with experimental data derived by Freyer et al. [36]. The diameter of the simulated tumour spheroid at the onset of necrosis has been shown to be practically the same as the experimental one (400 μm). The difference between the experimental and the simulated extent of the necrotic core decreases with increasing spheroid size. It must also be stated that although the tumour cell size contributes to the formation of the spheroid diameter, it barely affects the extent of the simulated necrosis as a function of the spheroid diameter. The central necrosis depends mostly on the viable and the proliferating rim thickness (onset and slope value) as well as on the time duration of necrosis.

The upper panel in Fig. 9 shows an equatorial cross-section of the developing tumour. The various cell states (proliferating phases, G_0 phase, necrotic/apoptotic products) can be readily distinguished. An eventual asymmetric or non-spherical formation of the tumour does not only differentiate the prediction from the cultured spheroid, but also affects the fraction of the tumour that is able to divide (growth fraction) and consequently the tumour growth rate. Since the spheroid symmetry significantly depends on the algorithms used for both tumour expansion and shrinkage, special attention has been paid to their formulation. Cross-sections normal to any coordinate axis are similar to the sections shown in Fig. 9, upper panel. Hence, the proposed novel algorithms describing the shifting of the cells in any direction in space have proved

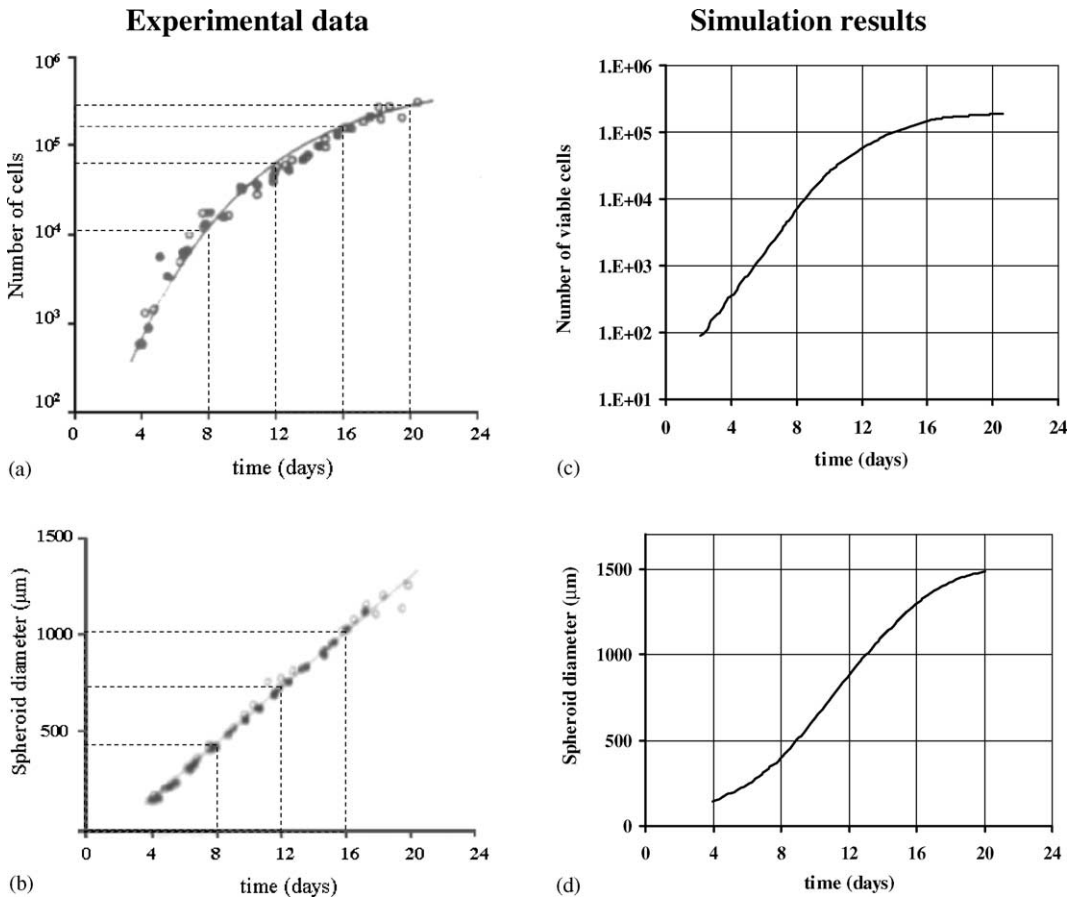

Fig. 6. Volumetric growth (a and c) and spheroid diameter (b and d) of the multicellular EMT6/Ro tumour spheroid as a function of time. (a) and (b) Experimental curves as appeared in Freyer et al. [36] (with permission) (c) and (d) prediction of the suggested simulation model.

to be able to form a spherical tumour. In this way the slightly hexagonal shape caused by the shifting in one of the six orthogonal directions of the cubic mesh has been overcome [19,15].

6.2. Tumour response to irradiation

According to [3] the radiation dose under hypoxia producing the same level of biological effect as the dose under aerobic conditions is equal to the latter multiplied by a factor, called the oxygen enhancement ratio (OER). This observation can be formulated as

$$S_{G_0}(\mathrm{OER}\cdot d) = S_P(d) \tag{6}$$

and leads to

$$\exp\left[-(\alpha_{G_0}\mathrm{OER}\cdot d + \beta_{G_0}(\mathrm{OER}\cdot d)^2)\right] = \exp\left[-(\alpha_P d + \beta_P d^2)\right], \tag{7}$$

where S_{G_0} is the surviving fraction of the hypoxic cells and S_P the surviving fraction of the proliferating cells after absorption of dose d according to the LQ model. The different pairs of α and β values modelling differences in radiosensitivity are defined in Section 4.4.

Eq. (7) can be satisfied in either of the following two ways: first by assuming that the linear and the quadratic components contribute to the damage independently [26], i.e.

$$\begin{cases} \alpha_{G_0}\mathrm{OER}\cdot d = \alpha_P d \Rightarrow \dfrac{\alpha_{G_0}}{\alpha_P} = \dfrac{1}{\mathrm{OER}} \\ \beta_{G_0}(\mathrm{OER}\cdot d)^2 = \beta_P d^2 \Rightarrow \dfrac{\beta_{G_0}}{\beta_P} = \dfrac{1}{(\mathrm{OER})^2} \end{cases} \tag{8}$$

or second by assuming that the dose at which the linear contribution to damage equals the quadratic contribution is the same for aerobic and hypoxic cells. In the latter case, the following equation holds

$$\frac{\alpha_P}{\beta_P} = \frac{\alpha_{G_0}}{\beta_{G_0}} = \lambda \tag{9}$$

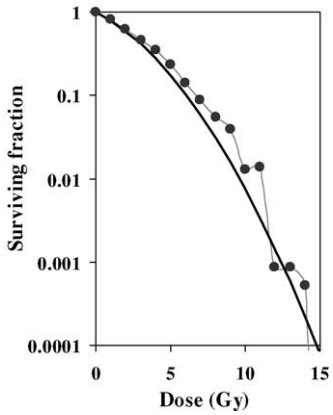

Fig. 7. Survival curve of the simulated EMT6 tumour spheroid irradiated before the development of hypoxia at 200 h. The points represent the mean values of two simulation runs each one having different seed of the random number generator. The solid line corresponds to the LQ survival probability of each proliferating cell.

Substituting Eq. (9) into (7) gives

$$\frac{a_{G_0}}{a_P} = \frac{\beta_{G_0}}{\beta_P} = \frac{\lambda + d}{\mathrm{OER}\lambda + (\mathrm{OER})^2 d}. \quad (10)$$

Using Eqs. (8) or (10) and for given α and β parameters, the S_{G_0} and β_{G_0} parameters for the G_0 phase can be calculated. Although the two equations express a different mechanism of biological damage, they both result in the same surviving fraction S_{G_0}. The OER for X-rays is around 3.0 for most cells [3].

Furthermore, cells in the S phase tend to be the most radioresistant out of the proliferating cells [32,33]. Classical experiments that have greatly supported this finding are those performed by Sinclair and Morton [37]. For the above-mentioned reason, the α_S and β_S values have been assumed smaller than the α_P and β_P values, respectively. It seems to be reasonable to assume the α_S and β_S values to be closer to the values of the radiobiological parameters of the rest of the proliferating cells than to the values of the parameters of the quiescent cells (e.g. $\alpha_S = 0.7a_P + 0.3a_{G_0}$, $\beta_S = 0.7\beta_P + 0.3\beta_{G_0}$). Estimates for the values of the and parameters of the α_P and β_P radiobiological LQ model have been derived from [23] ($\alpha_P = 0.21$, $\beta_P = 0.028$).

6.2.1. Results

A. Surviving fraction

In silico experiments have been performed to study the radiation dose-response curves of the simulated tumour spheroid. The spheroid diameter just before irradiation is ~190 μm. At this instant hypoxia has not yet developed. Fig. 7 shows the surviving fraction of the simulated EMT6 tumour spheroid in the dose range 0—15 Gy. A higher single dose irradiation induces killing of all viable cells. The surviving fraction is calculated by performing two different simulation runs with the same seed of the random number generator: one with and another one without irradiation. If we define survival as the ratio of the number of the viable cells surviving after irradiation over the number of the viable nonirradiated cells at the same instant, survival would be time dependent. We assume that the surviving fraction is defined when all radiation-induced damage mechanisms have been completed, i.e. when the survival ratio becomes minimum.

In Fig. 7, the survival probability of each proliferating cell as computed from the LQ model has been drawn with a solid line. The graph shows that the surviving fraction of the simulated tumour follows the irradiation survival probability of a single tumour cell. Furthermore, the irradiation of a tumour spheroid before the development of hypoxia satisfactorily simulates the irradiation under fully aerobic conditions in vitro of cells suspended from solid tumours. The predicted survival curve matches the experimental data for EMT6-Rw cells presented in [38] quite well. The surviving fractions of treated cells were calculated by normalizing their colony-forming ability to that of untreated cells plated during the same experiment [38].

B. Simulation of fractionated radiotherapeutic schemes

As the radiation response of EMT6 spheroids satisfactorily models the radiation response of EMT6 tumours [2], the following case is studied. A spheroid of diameter ~1500 μm where hypoxia is present is irradiated according to any one of the following common fractionated radiotherapeutic schemes:

- standard fractionation (2 Gy once a day, 5 days a week, 60 Gy in total);
- accelerated fractionation (2 Gy twice a day, 5 days a week, 60 Gy in total);
- hyperfractionation (1.2 Gy twice a day, 5 days per week, 72 Gy in total);
- hypofractionation (6 Gy once a day, 1 day a week, 60 Gy in total);

A time interval of 6 h between fractions has been assumed for all fractionation schemes. The spheroid has reached the above-mentioned diameter (i.e. 1500 μm) 600 h after the placement of a single tumour cell in the phase of mitosis at the centre of the discretizing mesh. Fig. 8 shows the

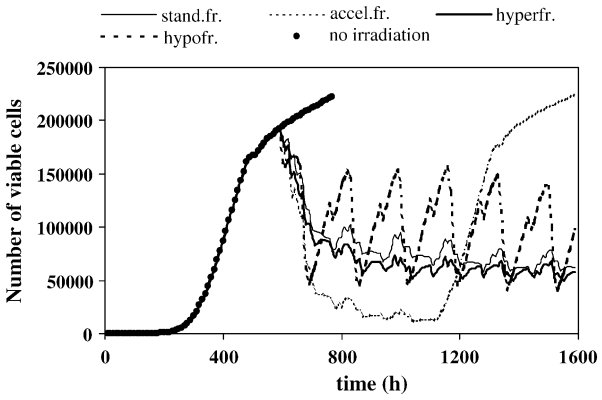

Fig. 8. The number of viable cells of an EMT6 tumour spheroid as a function of time if untreated as well as after the application of the standard fractionation (stand.fr.), accelerated fractionation (accel.fr.), hyperfractionation (hyperfr.) and hypofractionation (hypofr.) schemes. Irradiation begins 600 h after the placement of a tumour cell at the centre of the discretizing mesh.

number of viable cells of the EMT6 tumour spheroid as a function of time if untreated as well as after the application of any of the above described fractionation schemes. The rather periodical tumour cell number decrease caused by the dose fractions, as well as the repopulation effect of the weekend pause are easily distinguishable. No fractionation scheme succeeds in eliminating the tumour. Regrowth during radiotherapy is kept substantially low by accelerated fractionation and hyperfractionation. This is in accordance with experimental findings [3]. On the other hand, it is obvious — although not depicted in Fig. 8 — that the most effective scheme concerning scheme duration is hypofractionation. Similar simulation predictions have been presented by Ginsberg for the special case of exactly spherical tumours [23]. Nevertheless, these results cannot be generalized to every kind of tumour spheroid since the response to irradiation is strictly dependent on the duration of the cell cycle and the ratio.

Fig. 9 shows an equatorial section of the initially developing and subsequently responding to irradiation tumour. As an example, the accelerated fractionation scheme starting 600 simulated hours after the placement of a single tumour cell at the centre of the nutrient medium has been selected. The various cell states (proliferating cells, cells in the G_0 phase, cells in necrosis/apoptosis) can be readily distinguished. Fig. 10 has been produced using the visualisation package AVS/Express^{TM} 4.2 and depicts a 3D representation of the external surface of the tumour spheroid under consideration. The

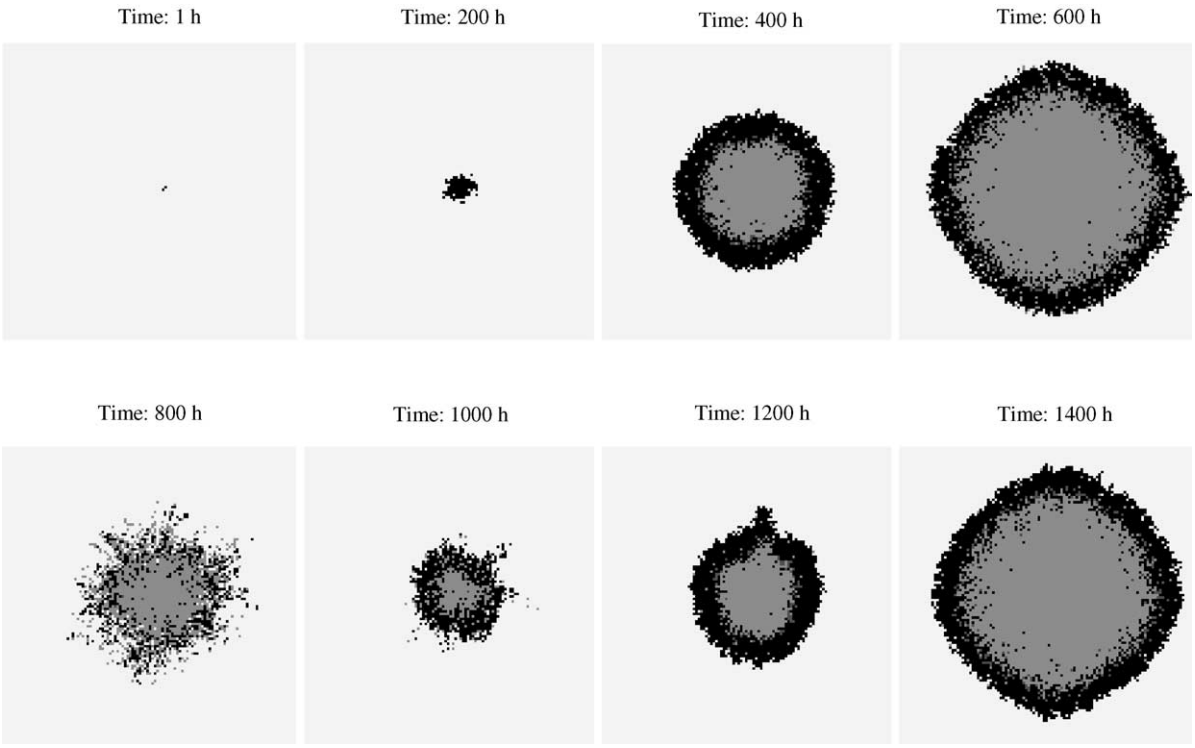

Fig. 9. Equatorial section of the initially developing (upper panel) and subsequently responding to accelerated fractionation tumour (lower panel). Irradiation begins 600 h after the placement of a tumour cell at the centre of the discretizing mesh. Grey scale code: black: cells in proliferating phases; dark grey: cells in G_0, light grey: cell death (necrotic, apoptotic), white: nutrient medium.

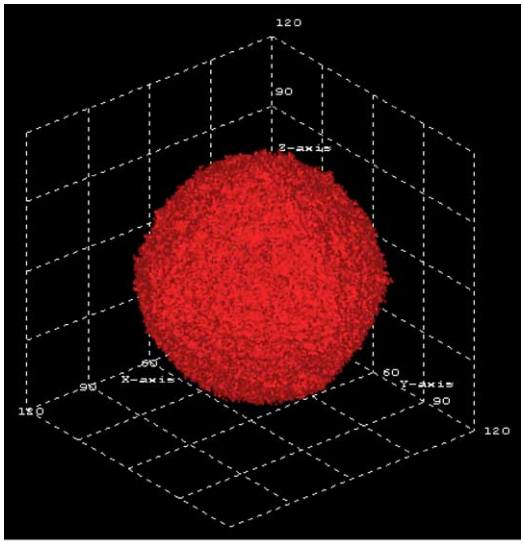

(a) Time: 600 h

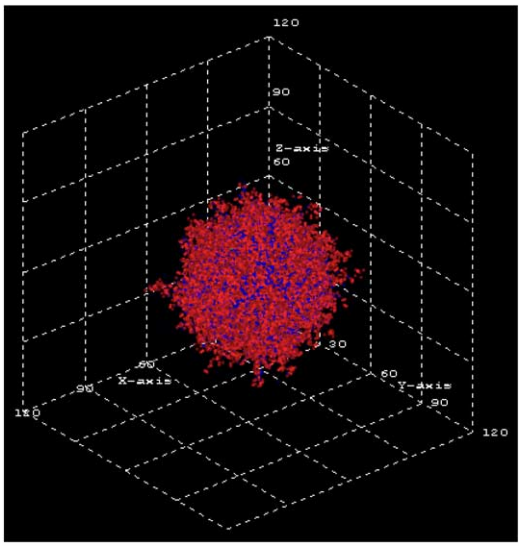

(b) Time: 800 h

Fig. 10. A 3D representation of the external surface of an EMT6 tumour spheroid using AVS/Express™ 4.2. The snapshots (a) just before and (b) 200 h after the beginning of the accelerated fractionation scheme (2 Gy twice a day, 5 days a week, 60 Gy in total). Colour code: light grey: proliferating cells; dark grey: products of cell necrosis/apoptosis. A virtual cut would reveal the green coloured cells in G_0 lying in the inner part.

two snapshots correspond just before and 200 h after the beginning of the accelerated fractionation scheme. Cell death is apparently much more pronounced in Fig. 10b.

6.3. Sensitivity analysis

The sensitivity of the model is analyzed against the most crucial parameters involved in tumour response to irradiation, i.e. the α and β values and the duration of the cell cycle phases. On the contrary, the specific way through which the cell will die, determined by the parameters quantifying interphase and mitotic cell death, does not seem to have a significant impact from the therapeutic point of view. The parametric analysis has been performed considering as the model output the number of surviving cells irradiated according to a given irradiation scheme, e.g. the standard fractionation scheme. The duration of each cell cycle phase is calculated as a percentage of the total cell cycle duration according to Salmon and Sartorelli [39]. The assumed durations of necrosis and apoptosis are shown in Table 1.

Firstly, the temporal response of a tumour spheroid with cell cycle duration 20 h has been evaluated by letting the values α_P vary in the range $0.2-0.6\,Gy^{-1}$ and $\beta_P = 0.1\alpha_P$ each time. The corresponding values α_S, β_S, α_{G_0}, β_{G_0} are calculated as previously described. A mean value of the number of viable cells in the range 200—800 simulated hours has been calculated. The predictions have demonstrated that the model is sensitive to increases in tumour radiosensitivity. The mean number of viable cells when $\alpha_P = 0.2\,Gy^{-1}$ is decreased by a factor of 0.48, 0.23, 0.09 and 0.03 when α_P is increased by a step of $0.1\,Gy^{-1}$, correspondingly.

Secondly, the radiobiological values have been kept constant, $\alpha_P = 0.4\,Gy^{-1}$ and $\beta_P = 0.04\,Gy^{-2}$, whereas the cell cycle duration has been considered to vary in the range 10—50 h. An increase in the cell cycle duration has similar effects on survival as an increase in radiosensitivity. Increasing cell cycle duration by a step of 10 h the mean number of viable cells compared to the mean number of viable cells with a cell cycle of 10 h is decreased by a factor of 0.22, 0.07, 0.04 and 0.04, respectively.

7. Lessons learned

The proposed simulation model is based on discrete spatiotemporal rules describing the (radio)biological behaviour of a 3D tumour spheroid instead of applying complex mathematical formulations. The novelty of the model basically refers to the following characteristics.

(i) The tumour structure (including the well oxygenated, the hypoxic and the necrotic layers) has been adapted to the experimental situation by exploiting published physiological data concerning oxygen, nutrient and cell death product diffusion. An excellent agreement of the predicted with the experimentally

observed extent of central necrosis supports the validity of the model.

(ii) A detailed cytokinetic diagram has been introduced, in which apparently all possible pathways in the cellular level leading to cell death have been incorporated. These pathways include interphase cell death via either spontaneous or radiation induced apoptosis, as well as mitotic cell death through either necrosis or apoptosis. Such a detailed cellular level model does not appear to have been presented in the literature as yet.

(iii) An extensive study of the statistical behaviour of the tumour growth algorithms has been performed and presented.

(iv) Cell shifting can take place along any random direction in the 3D space. This has been shown to lead to a remarkable preservation of the spheroidal shape of the tumours in accordance with experimental observations.

The model has been applied to the specific case of EMT6 tumour spheroids. Nevertheless, it can simulate the basic growth pattern characteristics that have been established for spheroids of many other cell types and cell lines [40], i.e. volume growth saturation, development of an outer proliferating rim and a growing necrotic centre. The validation of the tumour growth behaviour is a sine qua non task, as the assumptions describing the tumour geometry and the growth kinetics are critical for the tumour evolution after irradiation (shrinkage, regrowth, repopulation). Furthermore, simulations of the application of different fractionated schemes on a heterogeneous spheroid population offer a further tool for the extrapolation of the results to the in vivo case of solid avascular tumours. If the normal tissue response is ignored, the simulation predictions have shown that the accelerated fractionation scheme is the most effective during radiotherapy. However, after the completion of the scheme, the regrowth is very rapid. On the contrary, the hypofractionation scheme damages the tumour spheroid less during radiotherapy but keeps the cell number upper-bounded for a much longer period (10 weeks). The effectiveness of a fractionation scheme is as higher as the duration of the scheme is longer.

Qualitative and quantitative comparison of the simulated patterns with published experimental data concerning both tumour growth and survival after irradiation has provided reliable estimation on the accuracy of the model. As the simulation model is quite general, the cytokinetic and radiobiological properties of any particular type of tumour cells (able to form tumour spheroids in culture) can provide input to the computer program implementing the analysis presented. It should also be pointed out that as the radiobiological properties of a tumour (α and β parameters of the LQ model) depend on its genetic profile (e.g. p53 expression and mutation) an investigation of the macroscopic effects of the genetic data can be performed using the model. Furthermore, apart from the provision of the cytokinetic and radiobiological data for the specific tumour cells, no modifications to the code are in principle necessary. Obviously, experimental feedback should always be used in order to improve the reliability of the model.

8. Conclusions and future plans

The presented simulation model consists of a novel to a substantial degree biophysical approach and the application of currently available visualisation tools. The model can provide an efficient platform for gaining insight into the radiobiological mechanisms involved in tumour growth in vitro as well as during the avascular stages of in vivo tumour evolution. Optimisation of dose fractionation during radiation therapy by performing in silico experiments before the actual delivery of the radiation dose to the patient is the main practical target. A further application of the model might be the partial replacement of current expensive (in terms of both time and money) in vitro oncologic experiments by computer simulations.

Acknowledgements

The authors wish to thank Dr. Jim Freyer, Los Alamos National Laboratory, USA for his permission to redraw the experimental graphs that have been used to validate the simulation model. They also thank Dr. Roger Dale, Hammersmith Hospitals NHS Trust/Imperial College Faculty of Medicine, University of London for interesting discussions and his encouragement during the development of the model. They acknowledge the tireless computer hardware support by Dr. Pantelis Asvestas, National Technical University of Athens. Evangelia Zacharaki duly acknowledges the financial support of the Hellenic State Scholarship Foundation (IKY).

References

[1] G.S. Stamatakos, D.D. Dionysiou, E.I. Zacharaki, N. Mouravliansky, K.S. Nikita, N.K. Uzunoglu, In silico radiation oncology: combining novel simulation algorithms with cur-

rent visualization techniques, in: Proceedings of the IEEE, 2002, pp. 1764—1777.
[2] A.J. Franko, C.J. Koch, The radiation response of hypoxic cells in EMT6 spheroids in suspension culture does model data from EMT6 tumours, Radiat. Res. 96 (1983) 497—504.
[3] G. Steel, Basic Clinical Radiobiology, Arnold, London, UK 1997, pp. 15, 47—48, 52—57, 123—133, 153, 161.
[4] M. Santini, G. Rainaldi, P. Indovina, Multicellular tumour spheroids in radiation biology, Int. J. Radiat. Biol. 75 (1999) 787—799.
[5] R. Jostes, M. Williams, M. Barcellos-Hoff, T. Hoshino, D. Deen, Growth delay in 9L rat brain tumor spheroids after irradiation with single and split doses of X rays, Radiat. Res. 102 (1985) 182—189.
[6] J. Casciari, S. Sotirchos, R. Sutherland, Variations in tumor cell growth rates and metabolism with oxygen concentration, glucose concentration, and extracellular pH, J. Cell. Physiol. 151 (1992) 386—394.
[7] M. Santini, G. Rainaldi, Three-dimensional spheroid model in tumor biology, Pathobiology 67 (1999) 148—157.
[8] H. Lodish, D. Baltimore, A. Berk, S. Zipursky, P. Matsudaira, J. Darnell, Molecular Cell Biology, Scientific American Books, New York, 1995, pp. 1247—1294.
[9] W. Mueller-Klieser, Tumour biology and experimental therapeutics, Critical Rev. Oncol., Hematol. 36 (2000) 123—139.
[10] H.R. Withers, Biologic basis of radiation therapy, in: C.A. Perez, L.W. Brady (Eds.), Principles and Practice of Radiation Oncology, third ed., Lippincott-Raven, Philadelphia, 1998, pp. 79—118.
[11] J.F. Fowler, Review of radiobiological models for improving cancer treatment, in: K. Baier, D. Baltas (Eds.), Modelling in Clinical Radiobiology, Freiburg Oncology Series Monograph No. 2, Albert-Ludwigs-University, Freiburg, Germany, 1997, pp. 1—14.
[12] B. Jones, R. Dale, Mathematical models of tumour and normal tissue response, Acta Oncol. 38 (1999) 883—893.
[13] M. Marusic, Z. Bajzer, S. Vuk-Pavlovic, J.P. Freyer, Tumour growth in vivo and as multicellular spheroids compared by mathematical models, Bull. Math. Biol. 56 (1994) 617—631.
[14] W. Duechting, T. Vogelsaenger, Three-dimensional pattern generation applied to spheroidal tumour growth in a nutrient medium, Int. J. Biomed. Comput. 12 (1981) 377—392.
[15] G.S. Stamatakos, E.I. Zacharaki, M. Makropoulou, N. Mouravliansky, A. Marsh, K.S. Nikita, N.K. Uzunoglu, Modeling tumor growth and irradiation response in vitro—a combination of high-performance computing and web based technologies including VRML visualization, IEEE Trans. Inform. Technol. Biomed. 5 (2001) 279—289.
[16] G.S. Stamatakos, E.I. Zacharaki, N.K. Uzunoglu, K.S. Nikita, Tumour growth and response to irradiation in vitro: a technologically advanced simulation model, Int. J. Radiat. Oncol. Biol. Phys. 51 (Suppl. 1) (2001) 240—241.
[17] A.R. Kansal, S. Torquato, G.R. Harsh, E.A. Chiocca, T.S. Deisboeck, Simulated brain tumor growth dynamics using a three-dimensional cellular automaton, J. Theor. Biol. 203 (2000) 367—382.
[18] R. Wasserman, R. Acharya, A patient-specific in vivo tumour model, Math. Biosci. 136 (1996) 111—140.
[19] G.S. Stamatakos, D.D. Dionysiou, K.S. Nikita, N. Zamboglou, D. Baltas, G. Pissakas, N.K. Uzunoglu, In vivo tumor growth and response to radiation therapy: a novel algorithmic description, Int. J. Radiat. Oncol., Biol. Phys. 51 (Suppl. 1) (2001) 240.
[20] W. Duechting, Tumour growth simulation, Comput. Graphics 14 (1990) 505—508.
[21] S.A. Oprisan, A. Ardelean, P.T. Frangopol, Self-organization and competition in the immune response to cancer invasion: a phase-orientated computational model of oncogenesis, Bioinformatics 16 (2000) 96—100.
[22] W. Duechting, W. Ulmer, R. Lehrig, T. Ginsberg, E. Dedeleit, Computer simulation and modelling of tumour spheroid growth and their relevance for optimisation of fractionated radiotherapy, Strahlenther. Onkol. 168 (1992) 354—360.
[23] T. Ginsberg, Modellierung und Simulation der Proliferationsregulation und Strahlentherapie normaler und maligner Gewebe, Reihe 17: Biotechnik, Nr 140, Duesseldorf: Fortschritt-Berichte, VDI Verlag, 1996, pp. 103—107.
[24] A. Nahum, B. Sanchez-Nieto, Tumour control probability modelling: basic principles and applications in treatment planning, Physica. Medica. 17 (Suppl. 2) (2001) 13—23.
[25] M. Kocher, H. Treuer, Reoxygenation of hypoxic cells by tumour shrinkage during irradiation—a computer simulation, Strahlenther. Onkol. 171 (1995) 219—230.
[26] M. Kocher, H. Treuer, J. Voges, M. Hoevels, V. Sturm, R.P. Mueller, Computer simulation of cytotoxic and vascular effects of radiosurgery in solid and necrotic brain metastases, Radiother. Oncol. 54 (2000) 149—156.
[27] J.P. Freyer, R.M. Sutherland, Selective dissociation and characterization of cells from different regions of multicell tumour spheroids, Cancer Res. 40 (1980) 3956—3965.
[28] J.P. Freyer, R.M. Sutherland, Regulation of growth saturation and development of necrosis in EMT6/Ro multicellular spheroids by the glucose and oxygen supply, Cancer Res. 46 (1986) 3504—3512.
[29] A.C. Burton, Rate of growth of solid tumours as a problem of diffusion, Growth 30 (1966) 157—176.
[30] J. Landry, J.P. Freyer, R.M. Sutherland, A model for the growth of multicell tumour spheroids, Cell Tissue Kinet. 15 (1982) 585—594.
[31] C. Perez, L. Brady, Principles and Practice of Radiation Oncology, Lippincott-Raven, Philadelphia, 1998.
[32] E.J. Hall, Radiation and Cancer Biology. Part I: Systems and Principles, in: Proceedings of the ASTRO 43rd Annual Meeting Syllabi, The American Society for Therapeutic Radiology and Oncology, San Francisco, 4—8 November, 2001 (CD-ROM edition).
[33] A.J. Mundt, J.C. Roeske, R.R. Weichselbaum, Physical and biologic basis of radiation oncology, in: R.C. Bast, D.W. Kufe, R.E. Pollock, R.R. Weichelbaum, J.F. Holland, E. Frei (Eds.), Cancer Medicine, fifth ed., BC Decker Inc., Canada, 2000.
[34] W.C. Dewey, C.C. Ling, R.E. Meyn, Radiation-induced apoptosis: relevance to radiotherapy, Int. J. Radiat. Oncol. Biol. Phys. 33 (1995) 781—796.
[35] C.C. Ling, C.H. Chen, Z. Fuks, An equation for the dose response of radiation-induced apoptosis: possible incorporation with the LQ model, Radiother. Oncol. 33 (1994) 17—22.
[36] J.P. Freyer, R.M. Sutherland, A reduction in the in situ rates of oxygen and glucose consumption of cells in EMT6/Ro spheroids during growth, J. Cell. Physiol. 124 (1985) 516—524.
[37] W. Sinclair, R. Morton, X-ray and ultraviolet sensitivity of synchronized Chinese hamster cells at various stages of the cell cycle, Biophys. J. 5 (1965) 1—25.
[38] S. Rockwell, Absence of contact effects in irradiated EMT6-Rw tumours, Radiat. Res. 107 (1986) 375—381.
[39] S.E. Salmon, A.C. Sartorelli, Cancer chemotherapy, in: BG. Katzung (Ed.), Basic Clinical Pharmacology, eighth ed., The McGraw-Hill, New York, 2001, pp. 925—926.
[40] C. Nirmala, J.S. Rao, A.C. Ruifrok, L.A. Landford, M. Obeyesekere, Growth characteristics of glioblastoma spheroids, Int. J. Oncol. 19 (2001) 1109—1115.